# *Geophysical expression of elements of the Rio Grande rift in the northeast Tusas Mountains - Preliminary interpretations*

Benjamin J. Drenth, Kenzie J. Turner, Ren A. Thompson, V. J. S. Grauch, Michaela A. Cosca, and John P. Lee, 2011, pp. 165-176

*in:*

*Geology of the Tusas Mountains and Ojo Caliente*, Author Koning, Daniel J.; Karlstrom, Karl E.; Kelley, Shari A.; Lueth, Virgil W.; Aby, Scott B., New Mexico Geological Society 62nd Annual Fall Field Conference Guidebook, 418 p.

*This page is intentionally left blank to maintain order of facing pages.*

# GEOPHYSICAL EXPRESSION OF ELEMENTS OF THE RIO GRANDE RIFT IN THE NORTHEAST TUSAS MOUNTAINS - PRELIMINARY INTERPRETATIONS

BENJAMIN J. DRENTH, KENZIE J. TURNER, REN A. THOMPSON, V.J.S. GRAUCH, MICHAEL A. COSCA, AND JOHN P. LEE

[1]U.S. Geological Survey, MS 964, Federal Center, Denver, CO, 80225, bdrenth@usgs.gov

Abstract—New interpretations of the nature of the Rio Grande rift and pre-existing rocks in the northeast Tusas Mountains region are derived from new and existing gravity and aeromagnetic data. 12-15 mGal amplitude gravity lows are interpreted to mainly reflect large thicknesses of the upper Oligocene to upper Miocene, syn-rift Los Pinos Formation and possibly significant amounts of the Eocene El Rito Formation. The Broke Off Mountain sub basin, named after the location of its greatest inferred depth, is interpreted to be a ~40 km long and ~13 km wide structure elongated in a northwest trend at the western margin of the San Luis Basin. The sub basin is interpreted to contain a maximum combined thickness of 900-2300 m of the Los Pinos Formation and El Rito Formation, with the Los Pinos Formation constituting the majority of the section. Sub basin age is constrained to be older than 21.6 ± 1.4 Ma, the age of a Hinsdale Formation basalt flow that caps the Los Pinos Formation section at Broke Off Mountain. This age constraint and surface geology indicate a pre- and early-rift age. The structural fabric of the northeast Tusas Mountains region is dominated by northwest-trending normal faults, as indicated by geologic mapping and interpretation of aeromagnetic data. Preliminary analysis of the aeromagnetic data suggests that lineaments, possibly reflecting faulting, trend through volcanic rocks as young as Pliocene in age. If correct, these interpretations challenge commonly held beliefs regarding two stages in the structural style of rifting, where early (Oligocene-Miocene) rifting was characterized by broad, shallow basins bounded by northwest-trending faults and later (Miocene-Pliocene) rifting was characterized by deep, narrow basins bounded by north-trending faults. The Broke Off Mountain sub basin is a counter example of a pre- and early-rift, deep and narrow basin. We hypothesize that the Broke Off Mountain sub basin may represent a southward extension of the Monte Vista graben in Colorado, based on similarities in geophysical expression, stratigraphy, and its position at the western portion of the San Luis Basin.

## INTRODUCTION

The San Luis Basin is one of the northernmost major basins that make up the Rio Grande rift (Fig. 1). The western margin of the San Luis Basin, including the northeast Tusas Mountains of New Mexico, is commonly regarded as a simple structural hinge controlling the down-to-east half graben geometry of the San Luis Basin. Associated rift structures are correspondingly inferred to be minor, accommodating relatively small thicknesses of syn-rift sediments (e.g., Lipman and Mehnert, 1979; Tweto, 1979). A previous investigation of San Luis Basin subsurface geometry based on regional gravity data (Keller et al., 1984) interpreted a thickness of syn-rift sediments exceeding 1.5 km in the northeast Tusas Mountains, but did not recognize the region as part of the San Luis Basin.

In stark contrast to the high structural relief of the Sangre de Cristo Mountains and relatively well-defined sub basins of the eastern margin of the San Luis Basin (Keller et al., 1984; Brister and Gries, 1994; Kluth and Schaftenaar, 1994), structural reflection of rift tectonism on the western margin is geomorphically subdued. Establishing the temporal and spatial patterns of extensional faulting based on geologic mapping is limited by: 1) a paucity of deep sub-surface drill hole data, 2) relatively poor exposures of fault surfaces, especially in unconsolidated sediments, and 3) limited opportunity for stratigraphic correlation of dateable surfaces across fault boundaries.

Here we provide a new, preliminary geologic interpretation of previously mapped terrain in the northeast Tusas Mountains (Fig. 1), incorporating interpretations of recently acquired gravity and aeromagnetic data with geologic mapping and new argon geochronology on volcanic rocks. Specific goals include 1) estimating the thickness of low-density sediments and determining what that thickness distribution indicates about basin structure and temporal pattern of rifting, 2) identifying potential geophysical signatures of poorly constrained faults and/or fault zones, and 3) interpreting the geophysical signatures of selected volcanic units.

## GEOLOGIC BACKGROUND

The San Luis Basin is one of several en echelon basins forming the Rio Grande rift of New Mexico and Colorado. Basin subsidence in the region began ~28-26 Ma, following caldera forming eruptions of ash-flow tuffs from the Platoro caldera complex of the San Juan volcanic field, and coinciding locally with eruption of the ~25.6 Ma Amalia Tuff from the Questa caldera of the Latir volcanic field (Lipman, 1975a, b; Lipman and Mehnert, 1975; Thompson and Dungan, 1985; Lipman et al., 1986; Thompson and Machette, 1989; Thompson et al., 1991; Lipman et al., 1996; Lipman, 2007).

An initial, late Oligocene to early Miocene stage of rifting is commonly associated with northwest-trending faults, formation of broad, shallow basins within and beyond the modern boundaries of the rift, and emplacement of predominantly basaltic lavas of the Hinsdale Formation (Lipman and Mehnert, 1975; Lipman, 1981, 1983; Aldrich et al., 1986; Morgan et al., 1986; Thompson et al., 1991). After a period of quiescence, a later episode of more focused rifting from the late Miocene to the Quaternary is mainly responsible for north-trending faults, deep and narrow sub basins located along the eastern basin-bounding Sangre de Cristo fault zone, and widespread basaltic volcanism reflected in predominantly basaltic volcanic rocks of the Taos Plateau volcanic field (Lipman and Mehnert, 1979; Dungan et al., 1984; Morgan et al., 1986; Brister and Gries, 1994; Kluth and Schaftenaar, 1994; Drenth et al., 2010).

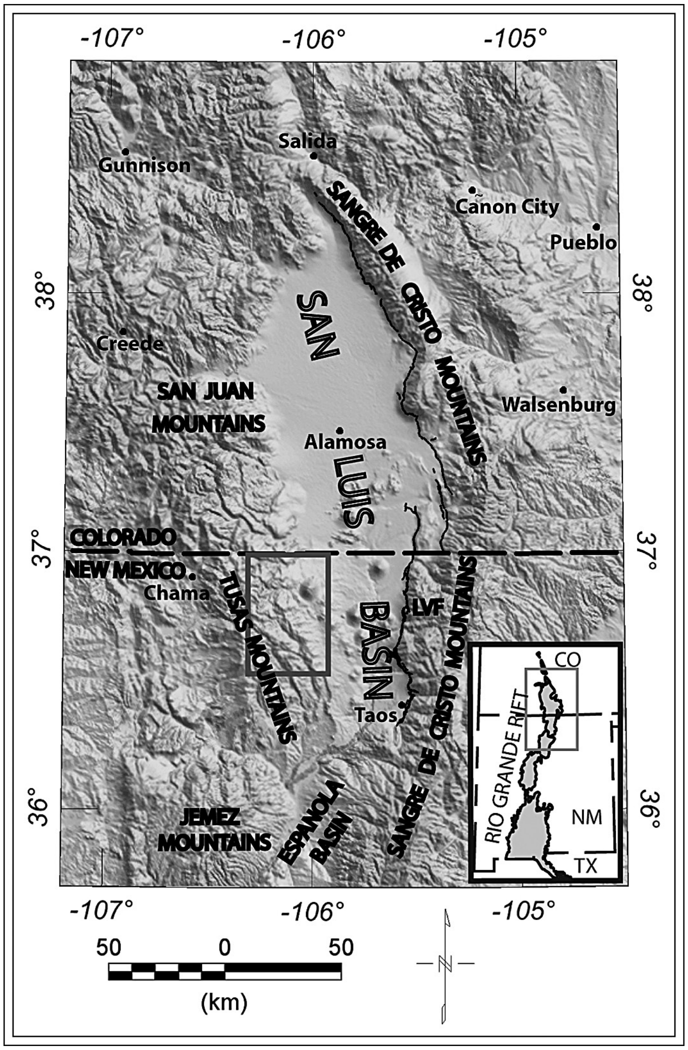


FIGURE 1: Physiography and geography of the San Luis Basin. Gray box defines area of this study. Sangre de Cristo fault zone shown as heavy black line. LVF, Latir volcanic field. San Juan volcanic field is largely coincident with San Juan Mountains. Inset map shows location of Fig. 1 in relation to the Rio Grande rift.

Geologic units in the study area are shown in Fig. 2 and Plate 6. Paleoproterozoic rocks (Xu) are the oldest rocks preserved in the study area (see Williams, 1991; Karlstrom et al., 2004, and references therein) and are uncomformably overlain by Eocene and Oligocene sedimentary and volcanic rocks (see Lipman, 2007; Maldonado and Kelley, 2009, and references therein). The Eocene El Rito Formation (Te) represents deposition in a north-trending Laramide-age syncline (Logsdon, 1981; Maldonado, 2008) and reaches a maximum exposed thickness of 135 m in the region (Manley et al., 1987). The Oligocene Conejos Formation (Tcf) consists of volcaniclastic sedimentary rocks, volcanic breccias, and lava flows originating from multiple volcanic centers in the southern San Juan volcanic field. The Oligocene Treasure Mountain Group (Tt), including the Chiquito Peak Tuff (Tcp), represent caldera-forming events from the Platoro caldera to the northwest in Colorado (Lipman, 1975b; Lipman et al., 1996). Dated at 28.41 Ma (Lipman et al., 1996), the Chiquito Peak Tuff is locally the youngest tuff of the San Juan volcanic field to be deposited prior to rift-related tectonism. Collectively, the volcanic rocks of the San Juan volcanic field thin southeastward, from a minimum thickness of 400 m (base not exposed) in the northwest portion of the area shown in Plate 6a (Manley, 1982a), to only 20-30 meters of the Treasure Mountain Group (Conejos Formation is absent) about 5 km south of Broke Off Mountain (Manley, 1982b; Wobus and Manley, 1982).

The Santa Fe Group is applied to syn-rift sediments overlying Oligocene volcanic rocks and volcaniclastic units in the Rio Grande rift (Spiegel and Baldwin, 1963; Ingersoll et al., 1990; Brister and Gries, 1994; Chapin and Cather, 1994). The upper Oligocene to upper Miocene Los Pinos Formation consists of volcaniclastic sediments derived from the San Juan and Latir volcanic fields (Butler, 1946, 1971; Manley, 1981). In the southern part of the map (Plate 6a) area Wobus and Manley (1982) describe a 45 m thick conglomerate composed of mainly Proterozoic clasts near the base of the Los Pinos Formation that may be correlative with the Oligocene Ritito Conglomerate (Maldonado and Kelley, 2009; Aby et al., 2010). Although no direct measurements are available for the Ritito Conglomerate, density and magnetic properties are not expected to be significantly different from the Los Pinos Formation. Given that, and its small thickness, the Ritito Conglomerate is expected to have little impact on the geophysical interpretations and is treated here as part of the Los Pinos Formation. Locally, the Los Pinos Formation reaches an exposed thickness of 350 m near Broke Off Mountain (Manley, 1982b). Initial extension and eastward tilting of the San Luis Basin is recorded by an angular unconformity cut across rocks of the San Juan volcanic field in the southeastern San Juan Mountains. This unconformity is overlain by an eastward-thickening section of the Los Pinos Formation, interlayered with basalts of the Hinsdale Formation (Lipman and Mehnert, 1975). The Los Pinos Formation is thus considered to occupy the same stratigraphic position as the Santa Fe Group (Lipman and Mehnert, 1975; Manley, 1981; Chapin and Cather, 1994; Smith et al., 2002; Smith, 2004). Others have challenged the notion that the Los Pinos Formation represents syn-rift sedimentation, arguing that deformation and sedimentation occurred prior to the inception of rift faulting, near magmatic centers rather than in rift basins proper (Ingersoll et al., 1990; Ingersoll and Cavazza, 1991; Large and Ingersoll, 1997; Ingersoll, 2001). For the purposes of subsurface modeling and interpretation, the Los Pinos Formation sediments are herein considered to be rift-basin fill.

The Hinsdale Formation consists of basaltic rocks that cap many ridges in the region (Figure 2 and Plate 6a). The onset of basaltic volcanism of the Hinsdale Formation (Thb) is considered to be coincident or nearly coincident with the inception of rifting. Published K-Ar ages on Hinsdale Formation lavas range from 27.7 Ma (Thompson et al., 1991) to 3.9 Ma (Lipman, 1975b; Lipman and Mehnert, 1975; Thompson and Lipman, 1994a). In this report, we restrict inclusion of basaltic lavas within the Hinsdale Formation to those older than the Pliocene. Whole rock K-Ar ages for Hinsdale lavas in the study area are as old as 24.6 ± 1.8 Ma on lavas directly west of San Antonio Mountain (referenced in Thompson and Lipman, 1994b, as H.H. Mehnert, unpublished

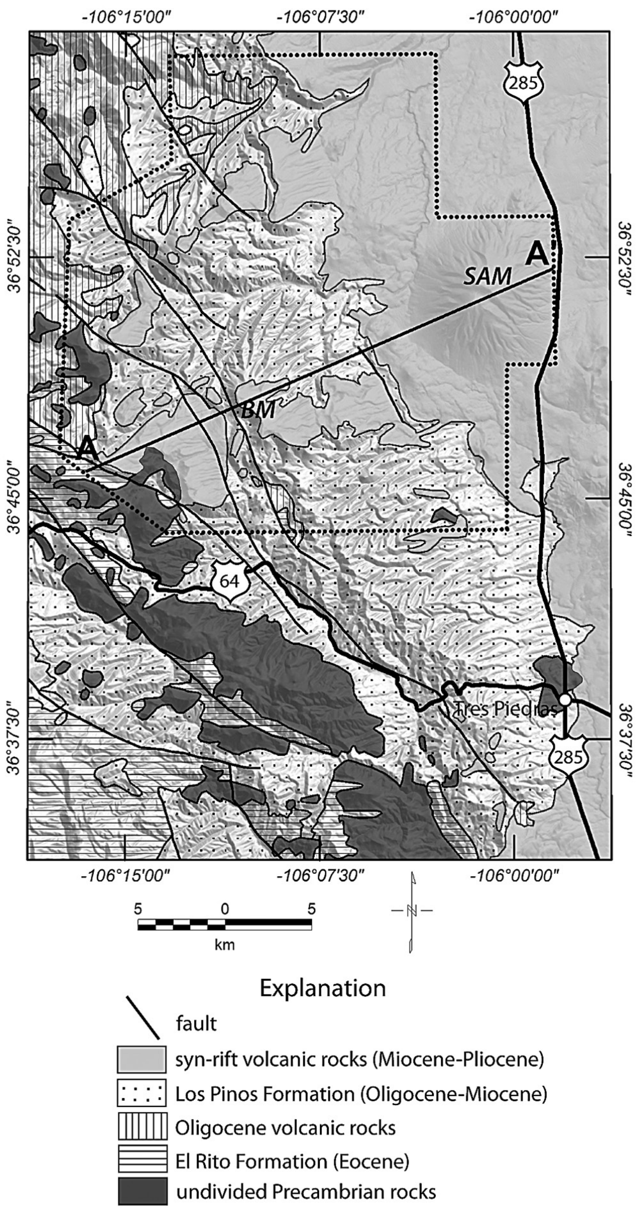


FIGURE 2: Simplified geologic map of the northeast Tusas Mountains region, modified from Anderson and Jones (1994) and Green and Jones (1997). Labels: BM, Broke Off Mountain; SAM, San Antonio Mountain. Area of detailed geologic map (Plate Xa) and aeromagnetic survey (Plate Y) shown by dotted line. Faults are shown as solid lines, but most are based on structures originally mapped as being only approximately located (e.g., Plate Xa).

data) and 21.6 ± 1.4 Ma at Broke Off Mountain (referenced in Thompson and Lipman, 1994b, as H.H. Mehnert, unpublished data, 1992). The youngest Hinsdale lava dated in the study area is 15.3 ± 0.8 Ma from a lava northwest of San Antonio Mountain (Thompson and Lipman, 1994a).

Pliocene volcanic rocks cover much of the eastern portion of the study area (Figure 2 and Plate 6a), including flows of the regionally extensive Servilleta Basalt and several other volcanic units of the ~6-2 Ma Taos Plateau volcanic field (Lipman and Mehnert, 1975, 1979; Dungan et al., 1984; Dungan et al., 1989; Appelt, 1998). Xenocrystic basaltic andesites erupted from multiple volcanic vents, identified by preserved cinder deposits. Thompson and Lipman (1994a) report a K-Ar age of 3.9 ± 0.4 Ma for basaltic andesite (Tbx) to the northwest of San Antonio Mountain. Preliminary $^{40}Ar/^{39}Ar$ geochronology (reporting 2σ error) indicates ages of 3.4 ± 0.1 Ma for the basaltic andesite of Cerritos de la Cruz (Tcx) and 2.9 ± 0.2 Ma for the basaltic andesite of Red Hill (Trx). San Antonio Mountain is composed primarily of dacitic lava flows erupted about 3.1 ± 0.1 Ma, underlain by andesite flows that may represent an earlier shield volcano (Thompson and Lipman, 1994a, b). Tholeiitic basalts of the Servilleta Basalt show a range in preliminary $^{40}Ar/^{39}Ar$ ages from 3.4 ± 0.2 Ma on a sample west of San Antonio Mountain to 2.5 ± 0.2 Ma on a sample southeast of San Antonio Mountain along U.S. Highway 285. Due to its protracted eruptive history and relatively large eruptive volume, the Servilleta Basalt lies stratigraphically above and below other Pliocene volcanic rocks at different localities in the study area.

Mapped faults in the northeast Tusas Mountains are dominantly northwest-trending, with both down-to-southwest and –northeast offsets (Fig. 2 and Plate 6a). Many of these faults were active after emplacement of the Hinsdale Formation, most notably a fault with ~200 m of down-to-southwest offset near the western margin of Broke Off Mountain, but more precise timing of faulting activity is poorly constrained. Geologic mapping (Plate 6a) shows a significant number of faults cutting early-rift (Oligocene and Miocene) rocks, such as the Los Pinos and Hinsdale Formations, with little to no faulting of Pliocene volcanic rocks. Very little information on bedding attitudes is available, but volcanic horizons are east dipping, with Oligocene and Miocene rocks having steeper dips (2-5º) than Pliocene rocks (1-2º).

## GEOPHYSICAL DATA AND METHODS

### Gravity Methods

Gravity anomalies reflect lateral variations of density, with gravity highs occurring over regions of relatively high densities, such as mountains composed of crystalline basement, and gravity lows occurring over large volumes of low-density materials, such as sediments. Large density contrasts between low-density basin-filling sediments, such as the Los Pinos Formation, and high-density pre-rift rocks make gravity data useful for defining the configuration of basins within the Rio Grande rift (Cordell, 1978; Keller et al., 1984; Daggett et al., 1986; Grauch et al., 2006; Grauch et al., 2009).

Regional-quality (1-5 km station spacing) gravity data were extracted from the PACES gravity database (Keller et al., 2006) that is maintained by the University of Texas at El Paso (http://gis.utep.edu/) and supplemented with the acquisition of 57 new stations in the northeast Tusas Mountains region during 2009 and 2010. Standard techniques (Simpson et al., 1986; Telford et al., 1990; Heywood, 1992; Blakely, 1995; Hinze, 2003; Jacoby and Smilde, 2009) were used to process the gravity data and calculate isostatic residual anomalies (Fig. 3) that reflect density variations of the upper crust.

A previous three-dimensional gravity model of the San Luis Basin (Keller et al., 1984) facilitated mapping of major tectonic elements and thickness of the Santa Fe Group. This work assumed a single density contrast (350 kg/m$^3$) between the Santa Fe Group and pre-rift rocks, and did not account for density variations within pre-rift rocks.

For this study we use additional gravity data and implement a more sophisticated approach to determine basin geometry: an inverse method (Jachens and Moring, 1990; Blakely and Jachens, 1991; Blakely, 1995) that focuses on separating the gravitational effect of low-density sediments from that of older, denser rocks. To accomplish this separation, the method adheres to independent constraints on basin-fill thickness and incorporates a user-defined density-depth function based on density logs for the basin fill (Table 1, Grauch et al., 2009) while also accommodating density variations of the pre-rift rocks. Results include an estimated thickness distribution of the low-density sediments (Fig. 4), and a computed gravity field attributed to pre-rift rocks. Locally, independent constraints come from mapped locations of outcropping Precambrian rocks (places where the thickness of low-density sediments is zero) (Manley, 1982a, b; Anderson and Jones, 1994; Green and Jones, 1997) and interpretations of drilling records (P. Bauer, written comm., 2009-2010) (Fig. 4).

The density-depth function used for the inversion (Table 1) is based on densities of rift-fill sediment, which does not account for the common occurrence of interbedded, syn-rift volcanic rocks. Basalts are common in the study area and denser than sediments. Their thickness distribution is estimated from geologic maps (Manley, 1982a, b; Anderson and Jones, 1994; Thompson and Lipman, 1994a, b; Green and Jones, 1997) and interpretation of well information. The gravitational effect of that distribution, as much as 2 mGal in the eastern portion of the study area, is calculated (Bott, 1960) and removed prior to performing the inversion and applying the density-depth function.

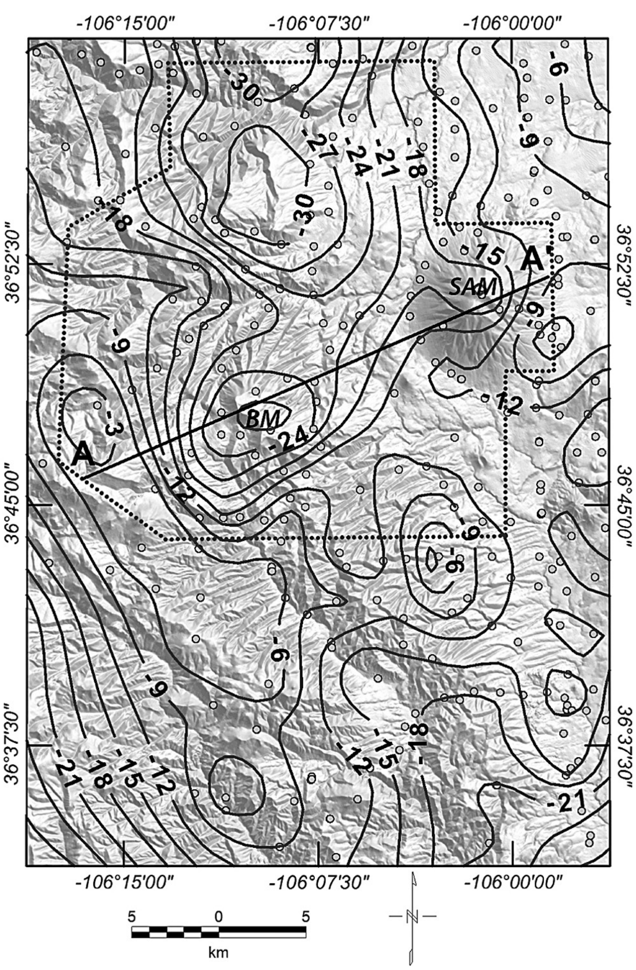


FIGURE 3: Isostatic residual gravity anomaly map of the study area. Gray dots are gravity station locations. Contour interval 3 mGal. Location of profile model A-A' shown. Labels: BM, Broke Off Mountain; SAM, San Antonio Mountain. Polygon defined by dotted line is extent of aeromagnetic survey.

### Aeromagnetic Methods

Aeromagnetic anomalies reflect spatial variations of total magnetization, the vector sum of induced and remanent magnetizations (Blakely, 1995). Induced magnetization is proportional to magnetic susceptibility and has the same direction as the present-day ambient field (inclination of 64 degrees, declination of 10 degrees in the study area). Remanent magnetization is related to the age and nature of a rock's formation and subsequent geologic history, and may be oriented in a different direction than the induced magnetization. Volcanic rocks normally carry a large-magnitude component of remanent magnetization, and are often referred to as being normally (magnetization directed parallel or sub-parallel to modern field) or reversely (magnetization directed antiparallel or sub-antiparallel to modern field) polarized. In regions with near-surface volcanic rocks and locally high topographic relief, magnetic anomalies can be produced in several different ways, depending on rock magnetic properties, volume and depth of the source, and relation to topography. In this region, aeromagnetic lows can be sourced by reversely polarized, highly magnetic rocks (generally represented by relatively large-magnitude magnetic lows), and weakly magnetized rocks (commonly represented by subtle, broad lows). Aeromagnetic highs can alternatively be interpreted as caused by normally magnetized rocks or magnetic rocks with induced magnetization that is much greater than the remanent magnetization. More complex terrain effects can be well developed along edges of magnetic rock units, such as truncated basalt flows that cap uplands or ridges.

During October, 2010, a high-resolution (200 meter flight-line spacing, 100 m above the ground) total-field aeromagnetic survey was flown over much of the northeast Tusas Mountains. A reduction-to-pole (RTP) transformation, a standard geophysical technique used to center anomalies over their sources (Baranov and Naudy, 1964; Blakely, 1995), was applied to the aeromagnetic data using the Earth's present-day field direction (Plate 7).

Aeromagnetic data are useful for detection of faults, in cases where there is suitable offset and magnetization contrast across a structure. In these cases, steep normal faults commonly produce

TABLE 1: Density-depth function used for gravity inversion (from Grauch et al., 2009).

| Depth (m) | Density (kg/cubic meter) |
|---|---|
| 0 - 1250 | 2170 |
| 1250 - 2750 | 2300 |
| 2750 - 3750 | 2380 |
| 3750 - | 2540 |

linear magnetic anomalies and/or breaks in anomaly patterns. These linear features can be enhanced in aeromagnetic maps by computation of the horizontal gradient magnitude (HGM), based on the principle that the largest-magnitude gradients are located over near-vertical magnetic property contrasts (Cordell and Grauch, 1985; Grauch and Cordell, 1987). The HGM and first vertical derivative (not shown) of the RTP aeromagnetic anomalies for the study area were calculated and used to interpret possible faulting patterns (Fig. 5), using the methods outlined by Grauch and Hudson (2007). Lineaments clearly related to terrain were not included in the interpretation. A potential pitfall is that magnetization contrasts other than faults, such as simple geologic contacts and boundaries of volcanic flows, have similar expressions and may have been mapped as well. Such errors of interpretation are best detected by inspection in the field, provided that the rocks are exposed.

Given that volcanic rocks normally carry strong magnetic remanence and constitute much of the terrain in the northeast Tusas Mountains, comparison of aeromagnetic anomalies with topography allows magnetic polarities to be inferred (Grauch and Keller, 2004). For example, a topographic high composed of volcanic rocks with a corresponding aeromagnetic low is an indication that those volcanic rocks are reversely polarized. An aeromagnetic high over the same feature would be an indication of normal polarity. Estimated magnetic properties, including polarities, are interpreted for selected volcanic and sedimentary units and displayed in Table 2.

## GEOPHYSICAL EXPRESSION OF GEOLOGIC FEATURES

### Basin Geometry

12-15 mGal amplitude gravity lows over the northeast Tusas Mountains region are interpreted to largely reflect relatively large thicknesses of low-density sediments. Geologically constrained inversion of the gravity data yields thickness estimates as great as 1500 m in the area of Broke Off Mountain (Fig. 4). Thickness estimates greater than 200 m extend 15 km north and 27 km southeast of Broke Off Mountain, for a total length of about 40 km. The width of this zone reaches a maximum of about 13 km. We name this region of thickened low-density sediments the Broke Off Mountain sub basin, after the location of its greatest estimated thickness.

Our preferred model has a maximum thickness of 1500 m (Fig. 4), given the underlying assumptions that the density-depth function (Table 1) is appropriate for the basin fill and the gravity field over exposed pre-rift rocks is representative of that over buried pre-rift rocks. To examine a wider range of possible models, we tested end-member scenarios based on reasonable density ranges for pre-rift rocks and the Los Pinos Formation. The results suggest the deepest part of the sub basin at Broke Off Mountain could range from 900 m to 2300 m in thickness.

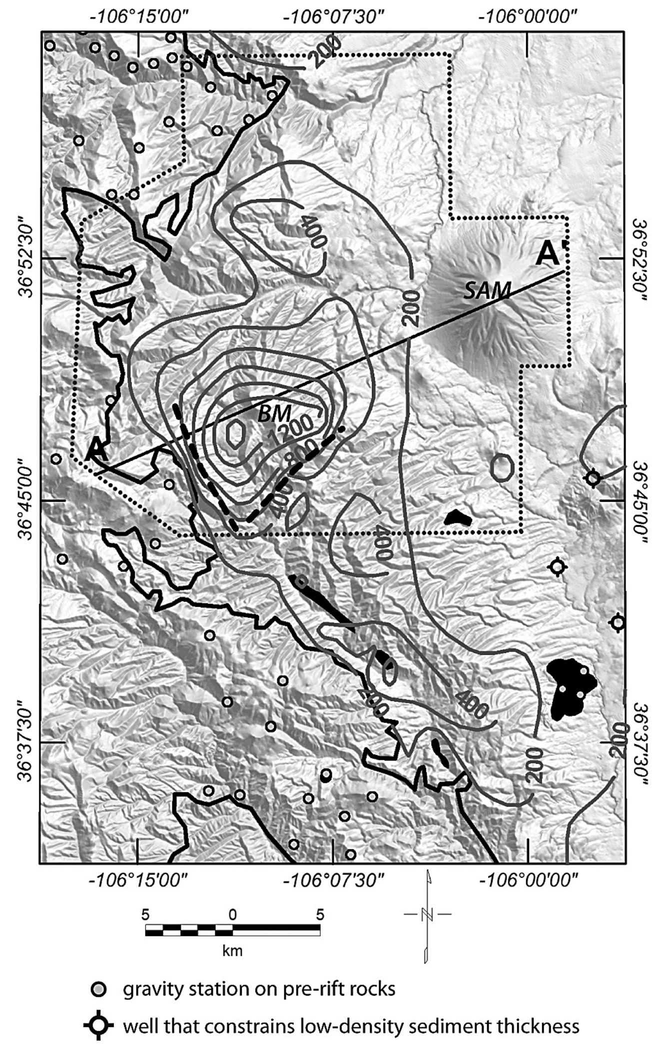


FIGURE 4: Constraints for three-dimensional gravity inversion and depth interpretations of low-density sediments. Heavy black line is boundary of the San Luis Basin, based on western extent of syn-rift rocks (from Fig. 2). Black polygons indicate outcropping Precambrian rocks within the basin, or places where the El Rito and Los Pinos Formation thicknesses are zero. Dark gray contours are estimated thickness of low-density sediments, contour interval 200 m. Heavy dashed lines indicate locations of inferred structures that control the deepest part of the Broke Off Mountain sub basin. Location of profile model A-A' shown. Polygon defined by dotted line is extent of aeromagnetic survey.

The gravity model reflects the thickness of low-density fill, including the syn-rift Los Pinos Formation. However, the pre-rift El Rito Formation and Treasure Mountain Group are likely to have densities close to 2170 kg/m$^3$ (Grauch and Hudson, 1987; Baldridge et al., 1994), the density assumed for the upper 1.25

TABLE 2: Physical properties interpreted/assumed for geologic units shown in the profile model A-A' (Plate Z).

| Unit (see Plate X) | Age (Ma) | Density (kg/ cubic meter)** | Magnetic polarity (N/R) | Magnetic susceptibility (SI units)*** | Estimated intensity of remanent magnetization (A/m)**** | Estimated Koenigsberger ratio (if >1, remanence dominated)** | Comment |
|---|---|---|---|---|---|---|---|
| Ts | 2.5-3.45 | 2700** | N* | 0.015* | 2* | >> 1 | |
| Td, low mag | 2.7-3.6 | 2300** | N | ? | 2-7 | > 1 | zone of attenuated magnetization near San Antonio Mtn summit |
| Td | 2.7-3.6 | 2400** | N | ? | 9-11 | >> 1 | |
| Ta | 2.7-3.6 | 2500** | N | ? | 2-9 | >> 1 | |
| Tcx vent | 3.4 | 2500** | R | ? | 0.5-4 | >> 1 | |
| Tcx | 3.4 | 2500** | N & R | 0.003-0.010 | 0.5-3 | 2-7 | Reversely polarized at location of profile |
| Thb | 21.6 ±1.4 | 2700** | N | 0.003-0.014 | 2-5 | 11-24 | At Broke Off Mtn. |
| Tlp | Oligocene to Miocene | 2170* | N | 0.012 | 0* | << 1 | Magnetic properties estimated from modeling |

*presumed based on expected rock properties and/or measurements outside study area
**estimated from rock type and/or modeling; Koenigsberger ratio is ratio of remanent magnetization intensity to induced magnetization intensity
***single value reported for presumed value, range reported for measured values
****estimated from modeling

km of the Los Pinos Formation (Table 1). The gravity model thus cannot distinguish them from the Los Pinos Formation within the sub basin, and there is a high probability that they are included in the reported thickness estimates. However, the thickness of the Treasure Mountain Group is small (thought to be < 100 m) in the vicinity of Broke Off Mountain (Manley, 1982b; Wobus and Manley, 1982), and the unit is probably insignificant at the scale of the gravity model unless it was deposited in a paleotopographic low not entirely filled by the underlying El Rito and Conejos Formations. The Conejos Formation is also likely present in the sub basin, although it is thin (~30 m) nearby (Manley, 1982b). It also has a higher estimated density of 2500 kg/m$^3$ (R. Gries, written comm., 2007) and is unlikely to be included in the thickness estimates for low-density rocks. Based on these observations, the El Rito Formation is thought to be the most volumetrically significant pre-rift unit included in thickness estimates for the Broke Off Mountain sub basin.

A conservative estimated thickness for the Los Pinos Formation is about 750 m under the deepest part of the sub basin, based on patterns of exposed thickness. Northwest of Broke Off Mountain, the thickness increases southeastward from about 135 m to 300 m over a distance of 3 km between locations B and C (Plate 6a). Projecting that rate of thickness increase 8.2 km from location B to D (Plate 6a) results in a thickness increase of ~450 m, in addition to the 300 m exposed at location 2, totaling 750 m below Broke Off Mountain.

The close proximity of the deepest part of the sub basin at Broke Off Mountain to the nearest outcrops of pre-rift rocks and areas of small (< 200 m) estimated thickness indicates that significant structural relief is present between those locations (Fig. 4). We thus infer that individual normal faults, groups of closely spaced normal faults, or zones of steep pre-basin paleotopographic slopes must be present that locally control the southwest and southeast boundaries of the sub basin (Fig. 4). These features represent the sub basin bounding structures that we interpret with the greatest confidence. However, additional bounding structures are likely present, as suggested by the gravity model and the aeromagnetic data.

### Aeromagnetic Expression of Structures

Possible faults interpreted from the aeromagnetic data show a pattern dominated by northwest-striking lineaments, and some northeast-striking lineaments (Fig. 5). Some of the aeromagnetic lineaments may represent flow boundaries or non-faulted contacts, but a reasonable interpretation based on the HGM map (Fig. 5) suggests that the majority represent faults. The northwest trends are similar to the mapped pattern of faults (Plate 6a), although the precise locations of most mapped faults do not correspond well to aeromagnetic lineaments. The discrepancy may be caused by a lack of magnetization contrast between rocks juxtaposed at the faults, imprecision in the locations of mapped faults (most are only approximately located), lack of dissection of Pliocene and younger faults (helpful in mapping faults), or the aeromagnetic expression is of faults in Precambrian rocks concealed under younger, unfaulted strata.

The possible difference in density of faulting between early-rift (Oligocene-Miocene) and late-rift (Pliocene to Pleistocene) rocks (Plate 6a) is not supported by the aeromagnetic interpretation, which on the contrary shows consistent patterns of linea-

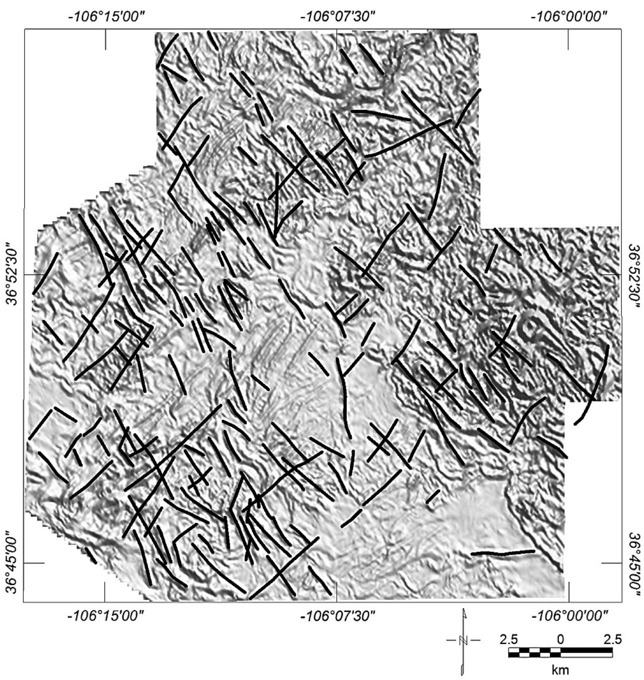


FIGURE 5: Horizontal gradient magnitude (HGM) of reduced-to-pole aeromagnetic anomalies (Plate Y) in shaded relief, illumination from the northeast. Black lines are drawn over lineaments interpreted to be possible faults.

ments trending through both groups of syn-rift rocks. Preliminary magnetic source depth estimates indicate that the interpreted faults are mainly shallow and thus lie within outcropping or shallowly buried volcanic and sedimentary rocks.

A prominent northeast-trending aeromagnetic gradient, separating high values on the southeast from lower values on the northwest (Plate 7, Fig. 5), is coincident with the southeast margin of the deepest part of the sub basin (heavy dashed line in Figure 4). Weakly magnetized El Rito Formation and thin (< 10 m) Chiquito Peak Tuff crop out there, implying that the likely source of the high anomaly values on the southeast is shallow, strongly magnetized Precambrian rock. Perhaps the gradient represents a northeast-trending bounding structure with Precambrian rocks at a lower elevation on the northwest under the deepest part of the sub basin. This explanation is supported by magnetic depth analysis (not shown) that indicates strongly magnetized rocks are at depths of 100-250 m at a location 1-2 km southeast of the gradient (Fig. 4), consistent with the ~200 m thickness of low-density sediments estimated from the gravity inversion.

## Profile Model

To quantitatively display and assess the interpreted geologic relationships, a 2.5-D gravity and magnetic model along profile A-A' (Plate 8) was constructed using the preferred gravity inversion results as a starting point. The profile location was chosen to most effectively capture the main geologic features of interest in the study area.

Because we want to focus on the geophysical effects of low-density rocks, we first construct an equivalent density and magnetic model to account for the geophysical anomalies produced by dense pre-rift rocks (largely Precambrian). Because the subsurface configuration and physical properties of dense pre-rift rocks are unknown, the best estimates on the gravity field associated with them come from the gravity inversion itself. The equivalent model is constructed in a way that matches the gravity field resulting from the inversion, as well as the relatively long-wavelength (i.e., due to buried, deep, and/or broad anomaly sources) aeromagnetic anomalies. In other words, the equivalent model serves as a proxy to compute and remove the effects of the poorly understood dense pre-rift rocks, leaving the effects of low-density rocks. Arbitrary, yet geologically plausible, densities and magnetic susceptibilities are assigned to vertically bounded zones that are 7-8 km thick until the gravity field due to dense pre-rift rocks and long-wavelength magnetic anomalies are matched.

The next step is to develop the geometry of the base of the low-density sediments. The results of the preferred gravity inversion (Fig. 4) provide a robust first approximation of the low-density sediment thickness, and subsequent adjustments to the model result in only small differences (<10%) between the inversion results and the final model (dotted line, Plate 8). The minor adjustments account for the effects of surficial volcanic rocks and correct for small errors in the fit to the gravity data. The final step is to build volcanic rocks into the model, honoring their surficial contacts and thicknesses shown on geologic maps (Manley, 1982b; Thompson and Lipman, 1994a, b), stratigraphic configuration (Plate 6b), and interpreted physical properties (Table 2).

The maximum thickness of the low-density sediments reaches nearly 1400 m along the profile model near the western topographic margin of Broke Off Mountain. The overall shape of the sub basin at the location of the profile is hypothetically that of a half-graben controlled by the major fault at its southwestern boundary, assuming that the other inferred faults in the model (see below) are minor structures. It is not clear whether or not the other margins of the sub basin are fault controlled. Other vertically extensive and relatively significant faults are inferred from changes in the low-density sediment thickness that correspond to locations of faults mapped on the surface or inferred from the aeromagnetic data (Plate 8). Very little is known about the age and amount of displacement on these faults, or the dips of the Los Pinos Formation; thus the structural interpretation presented in the model is only one plausible scenario.

Volcanic rocks produce the largest aeromagnetic anomalies along the profile model. An extraordinarily large (~4000 nT amplitude) high with a central low (Plate 7) lies over San Antonio Mountain. The andesite and dacite that form the mountain (Plate 6) can explain most of the anomaly, based on their outcrop geometry. The central low is best explained by a zone of reduced magnetization of normal polarity that lies within the center of the mountain. The geologic nature and vertical extent of this zone are unknown, although the horizontal boundaries are well-constrained by aeromagnetic gradients (Figs. 5, 6). Basalts of the Hinsdale Formation produce anomalies of variable amplitude in the region, suggesting that they have variable magnetic proper-

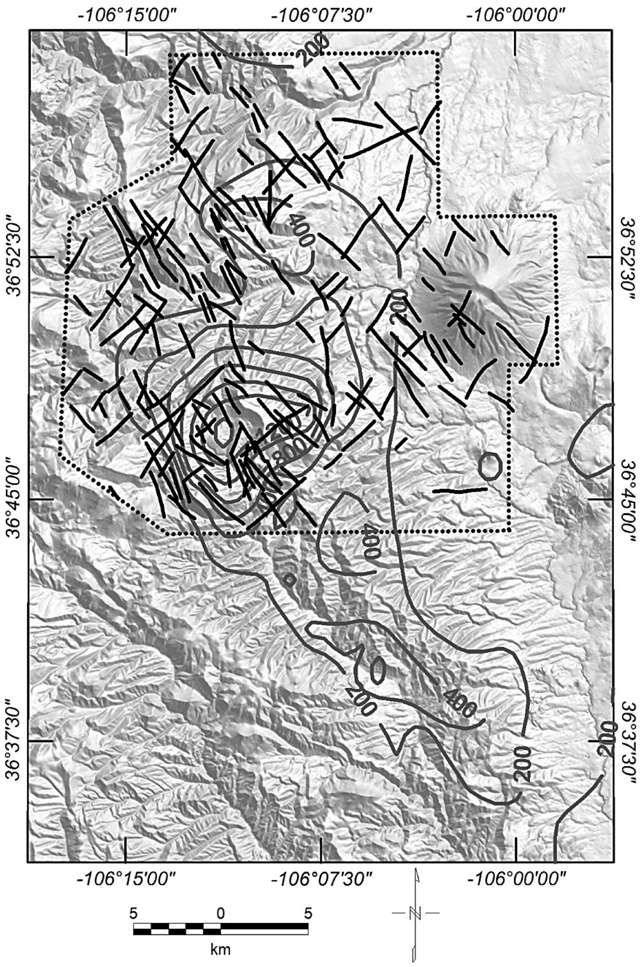


FIGURE 6: Summary of new geophysical interpretations resulting from this study. Dark gray contours are estimated thickness of low-density sediments, contour interval 200 m. Black lines are possible faults as interpreted from aeromagnetic data. Polygon defined by dotted line is extent of aeromagnetic survey.

ties and/or thickness. Along the profile, the Hinsdale Formation is known to be thin (from geologic mapping) and has relatively low magnetic susceptibilities (from limited field measurements), yet it produces highs of 100-200 nT. Modeling indicates these basalts must have strong normal-polarity magnetic remanence (Table 2) to produce the observed anomalies. Reversely polarized basaltic andesites (unit Tcx) produce the high-amplitude aeromagnetic lows observed about 6 km southwest of San Antonio Mountain (Plates Xa, Y, Z).

A ~900 nT aeromagnetic high near the southwestern end of profile A-A' (Plate 7) cannot be directly correlated with any units that crop out at the surface. The sub-circular shape and high amplitude of the anomaly are indicative of a source with a thickness that is large compared to its width, as opposed to a thin, tabular-shaped source (such as a volcanic flow). The most logical interpretation of this anomaly is a pluton, which must be buried (because it is not mapped). There are several Precambrian plutons in the region, and we thus speculate that the source of the aeromagnetic high is a pluton of likely Precambrian ancestry. The physical properties of the source are not known, but modeling with a high magnetic susceptibility (0.07 SI units) yields a body that is over 1 km thick.

## DISCUSSION

We regard the Broke Off Mountain sub basin to have formed initially prior to deposition of the Eocene El Rito Formation, yet to mainly be an early syn-rift sub basin, based on inferred thicknesses of sediments that fill it. An early Miocene minimum age of the sub basin is established by 21.6 ± 1.4 Ma Hinsdale Formation capping Los Pinos Formation at Broke Off Mountain, and lack of major offset of Hinsdale Formation directly above what is thought to be a major bounding structure at its southwestern margin (Plate 8). A minimum thickness estimate of 750-800 m for the Los Pinos Formation, based on geologic mapping, is greater than both the local maximum exposed thickness of 135 m for the Eocene El Rito Formation and the maximum thickness of buried Eocene strata in other parts of the region (see below). The combined thickness of these two units is close to the minimum thickness estimate of 900 m from the gravity inversion. Given that the Los Pinos Formation is the stratigraphic equivalent of rift-related sediments, we consider the Broke Off Mountain sub basin to be part of the larger, syn-rift San Luis Basin.

The sub basin shares important characteristics with the Monte Vista graben (Brister, 1990; Brister and Gries, 1994), located in the western part of the northern San Luis Basin in Colorado: 1) Both contain, or are inferred to contain, Eocene sediments, volcanic rocks of the San Juan volcanic field, and syn-rift sediments. 2) Both produce generally north-trending gravity lows that reflect thick, low-density sedimentary fill (Keller et al., 1984). 3) Both are located at the western margin of the larger San Luis Basin. The Broke Off Mountain sub basin is a smaller structure, with a maximum thickness of 900-2300 m and width of 13 km, compared to a thickness of 3 km and width of 25 km for the Monte Vista graben. We hypothesize that the Broke Off Mountain sub basin forms the southern tip of the Monte Vista graben.

The Broke Off Mountain sub basin may contain a greater thickness of the El Rito Formation than what crops out nearby (135 m). Eocene rocks are as much as 643 m thick in boreholes in the Monte Vista graben (Brister, 1990), and a comparable accumulation cannot be ruled out near Broke Off Mountain. A total combined thickness for the El Rito and Los Pinos Formations of ~1500 m is geophysically reasonable. Significant buried thicknesses of the Conejos Formation and Treasure Mountain Group are also possible, although these units thin dramatically from the northwest to south of Broke Off Mountain, where only 20-30 m of the Treasure Mountain Group (including the Chiquito Peak Tuff) are exposed and the Conejos Formation is absent.

The boundaries of the Broke Off Mountain sub basin are difficult to interpret, due to poor exposures of faults and lack of information on timing of slip. Thus, the relative roles of paleotopography, pre-rift faulting, and syn-rift faulting in sub basin formation are generally difficult to separate from each other. However, two exceptions exist. First, the normal fault at the western topographic margin of Broke Off Mountain (Plate 6a) offsets basalt of the Hinsdale Formation ~200 m (e.g., Plate 8), indicating that it is a syn-rift structure. The fault also appears to form the northeast boundary of the deepest part of the sub basin (note 1400 m contour, Fig. 4), suggesting it was active during sedimentation. Second, the northwest-trending structure inferred to form the southwest margin of the deepest part of the sub basin (Fig. 4) is located near northwest-trending faults mapped on the surface (Plate 6a) and shallow structures mapped from the aeromagnetic data (Figs. 5, 6), suggesting syn-rift slip. However, slip must have predated emplacement of the Hinsdale Formation, because the inferred basin bounding structure is not associated with major offset of it.

Structural trends inferred from aeromagnetic data and the gravity inversion are consistent with the pervasive northwest-trending fabric apparent on existing geologic maps (Plate 6a and Fig. 6). Northwest-trending faults are often assumed to reflect early-rift deformation. However, a large number of aeromagnetic lineaments caused by shallow sources trend northwest through Pliocene volcanic rocks, suggesting northwest-trending faults that post-date emplacement of those rocks and are associated with the later stage of rifting. Faulting may have been active episodically from the Eocene to the Quaternary. A significant number of northeast-trending lineaments are evident in the aeromagnetic data (Fig. 6), and the inferred sub basin-controlling structure under the southeast margin of Broke Off Mountain also trends northeast (Fig. 4). The significance of the northeasterly trends, present in both the gravity inversion results and the aeromagnetic data, is not understood, and may relate to pre-rift tectonic activity. However, inferred patterns of faulting in syn-rift rocks elsewhere in the San Luis Basin display a similar style, with both northwest and northeast trends (e.g., Ruleman et al., 2007). We consider the structural interpretation presented here (Plate 8) to be plausible, yet is only one possible solution, given the lack of information on faulting and dips of the Los Pinos Formation.

The interpretation of a narrow sub basin with a large thickness of early syn-rift sediments and possibly steep boundary structures is contrary to the common assumption that early rift basins were broad and shallow, and the interpretation (e.g., Ingersoll et al., 1990) that fault-bounded basins did not yet exist at the time of Los Pinos Formation sedimentation.

## CONCLUSIONS

Interpretations of basin structure in the northeast Tusas Mountains challenge commonly-held assumptions about the nature of the early Rio Grande rift. A ~40 km long, ~13 km wide, previously unrecognized structural depression, herein named the Broke Off Mountain sub basin, in the northeastern Tusas Mountains is interpreted to contain at least 750 m of the syn-rift Los Pinos Formation, with possibly significant amounts of Eocene rocks (Fig. 6). We regard the Broke Off Mountain sub basin to be part of the larger San Luis Basin, and hypothesize that it is a southern extension of the pre- and syn-rift Monte Vista graben recognized within the San Luis Basin in Colorado. The sediments filling the sub basin are older than 21.6 ± 1.4 Ma, the age of basalt of the Hinsdale Formation that crops out at the summit of Broke Off Mountain, and likely as old as Eocene. The sub basin thus likely represents a narrow, deep, pre- and early-rift structure, challenging the conventional belief that early-rift basins were broad, shallow features.

Numerous aeromagnetic lineaments, considered to mainly represent patterns of faulting, lie along northwest trends (Fig. 6), consistent with trends revealed by geologic mapping and commonly assumed to reflect early-rift deformation styles. However, inferred faults with northwest trends also cut Pliocene volcanic rocks, suggesting that faulting along northwest trends was not confined to early stages of rifting. Northeast trending lineaments are also apparent, and both trends are reflected in inferred structures that bound either side of the southern Broke Off Mountain sub basin. However, little information on precise fault locations and timing of slip is available, making it generally difficult to sort out the relative contributions of paleotopography, pre-rift faulting, and syn-rift faulting.

## ACKNOWLEDGMENTS

This work was supported by the National Cooperative Geologic Mapping and Mineral Resource Programs of the U.S. Geological Survey. The aeromagnetic survey was funded by the U.S. Geological Survey Crustal Geophysics and Geochemistry Science Center. Carson National Forest staff, particularly John Grasso, provided critical support to the gravity data collection effort. We thank Krystal Pearson, Michael Wussow, and Lauren Howell for assisting with gravity data acquisition. We acknowledge helpful reviews by Robert Horton and Cal Ruleman.

## REFERENCES CITED

Aby, S., Karlstrom, K.E., Koning, D.J., and Kempter, K., 2010, Preliminary geologic map of the Las Tablas Quadrangle, Rio Arriba County, New Mexico: New Mexico Bureau of Mines and Mineral Resources Open-File Geologic Map 200, 1:24,000 scale.

Aldrich, M.J., Chapin, C.E., and Laughlin, A.W., 1986, Stress history and tectonic development of the Rio Grande rift, New Mexico: Journal of Geophysical Research, v. 91, p. 6199-6211.

Anderson, O.J., and Jones, G.E., 1994, Geologic Map of New Mexico: New Mexico Bureau of Mines and Mineral Resources, Open-file Report 408-A and B, Geologic map and 15 magnetic disks, 1:500,000 map.

Appelt, R.M., 1998, 40Ar/39Ar geochronology and volcanic evolution of the Taos Plateau volcanic field, northern New Mexico and southern Colorado [Master's thesis]: Socorro, New Mexico Tech.

Baldridge, W.S., Ferguson, J.F., Braile, L.W., Wang, B., Eckhardt, K., Evans, D., Schultz, C., Gilpin, B., Jiracek, G.R., and Biehler, S., 1994, The western margin of the Rio Grande rift in northern New Mexico: an aborted boundary?: Geological Society of America Bulletin, v. 106, p. 1538-1551.

Baranov, V., and Naudy, H., 1964, Numerical calculation of the formula of reduction to the magnetic pole: Geophysics, v. 29, p. 67-79.

Blakely, R.J., and Jachens, R.W., 1991, Regional study of mineral resources in Nevada-- Insights from three-dimensional analysis of gravity and magnetic anomalies: Geological Society of America Bulletin, v. 103, p. 795-803.

Blakely, R.J., 1995, Potential Theory in Gravity and Magnetic Applications, Cambridge University Press, 441 p.

Bott, M.H.P., 1960, The use of rapid digital computing methods for direct gravity interpretation of sedimentary basins: Geophysical Journal of the Royal Astronomical Society, v. 3, p. 63-67.

Brister, B.S., 1990, Tertiary sedimentation and tectonics: San Juan sag-San Luis basin region, Colorado and New Mexico [Ph.D. thesis]: Socorro, New Mexico, New Mexico Institute of Mining ang Technology.

Brister, B.S., and Gries, R.R., 1994, Tertiary stratigraphy and tectonic development of the Alamosa basin (northern San Luis Basin), Rio Grande rift, south-central Colorado, *in* Keller, G.R., and Cather, S.M., eds., Basins of the Rio Grande Rift: Structure, Stratigraphy, and Tectonic Setting: Boulder, Geological Society of America Special Paper 291, p. 39-58.

Butler, A.P., Jr., 1946, Tertiary and Quaternary geology of the Tusas-Tres Piedras area, New Mexico [Ph.D. dissertation]: Cambridge, Harvard University, 188 p.

—, 1971, Tertiary volcanic stratigraphy of the eastern Tusas Mountains, southwest of the San Luis Valley, Colorado-New Mexico, *in* James, H.L., ed., Guidebook of the San Luis Basin: New Mexico Geological Society, 22nd Annual Field Conference Guidebook, p. 289-300.

Chapin, C.E., and Cather, S.M., 1994, Tectonic setting of the axial basins of the northern and central Rio Grande rift, *in* Keller, G.R., and Cather, S.M., eds., Basins of the Rio Grande Rift: Structure, Stratigraphy, and Tectonic Setting: Boulder, Geological Society of America Special Paper 291, p. 5-25.

Cordell, L., 1978, Regional geophysical setting of the Rio Grande rift: Geological Society of America Bulletin, v. 89, p. 1073-1090.

Cordell, L., and Grauch, V.J.S., 1985, Mapping basement magnetization zones from aeromagnetic data in the San Juan basin, New Mexico, *in* Hinze, W.J., ed., The Utility of Regional Gravity and Magnetic Anomaly Maps, Society of Exploration Geophysicists, p. 181-197.

Daggett, P.H., Keller, G.R., Morgan, P., and Wen, C.L., 1986, Structure of the southern Rio Grande rift from gravity interpretation: Journal of Geophysical Research, v. 91, p. 6157-6167.

Drenth, B.J., Grauch, V.J.S., and Thompson, R.A., 2010, Gravity investigation of the three-dimensional geometry of the San Luis Basin, northern Rio Grande rift- preliminary results: Geological Society of America Abstracts with Programs, v. 42, No. 5, p. 238.

Dungan, M.A., Muehlberger, W.R., Leininger, L., Peterson, C., McMillan, N.J., G., G., Lindstrom, M., and Haskin, L., 1984, Volcanic and sedimentary stratigraphy of the Rio Grande Gorge and the late Cenozoic geologic evolution of the southeastern San Luis Valley, *in* Baldridge, W.S., Dickerson, P.W., Riecker, R.E., and Zidek, J., eds., New Mexico Geological Society Guidebook, 35th Field Conference, Rio Grande Rift: Northern New Mexico, p. 51-57.

Dungan, M.A., Thompson, R.A., and Stormer, J.S., 1989, Rio Grande rift volcanism: northeastern Jemez zone, New Mexico, *in* Chapin, C.E., and Zidek, J., eds., Field excursions to volcanic terranes in the western United States, Volume 1: southern Rocky Mountain region: New Mexico Bureau of Mines and Mineral Resources Memoir 46, p. 435-486.

Grauch, V.J.S., and Cordell, L., 1987, Limitations of determining density or magnetic boundaries from the horizontal gradient of gravity or pseudogravity data: Geophysics, v. 52, p. 118-121.

Grauch, V.J.S., and Hudson, M.R., 1987, Summary of natural remanent magnetization, magnetic susceptibility, and density measurements from the Lake City caldera area, San Juan Mountains, Colorado: U.S. Geological Survey Open-File Report 87-182.

Grauch, V.J.S., and Keller, G.R., 2004, Gravity and aeromagnetic expression of tectonic and volcanic elements of the southern San Luis Basin, New Mexico and Colorado, *in* Brister, B.S., Bauer, P.W., Read, A.S., and Lueth, V.W., eds., New Mexico Geological Society Guidebook, 55th Field Conference, Geology of the Taos Region, p. 230-243.

Grauch, V.J.S., Sawyer, D.A., Minor, S.A., Hudson, M.R., and Thompson, R.A., 2006, Gravity and aeromagnetic studies of the Santo Domingo basin area, New Mexico, *in* Minor, S.A., ed., The Cerrillos Uplift, the La Bajada Constriction, and Hydrogeologic Framework of the Santo Domingo Basin, Rio Grande Rift, New Mexico, U.S. Geological Survey Professional Paper 1720, p. 62-86.

Grauch, V.J.S., and Hudson, M.R., 2007, Guides to understanding the aeromagnetic expression of faults in sedimentary basins: lessons learned from the central Rio Grande rift, New Mexico: Geosphere, v. 3, p. 596-623.

Grauch, V.J.S., Phillips, J.D., Koning, D.J., Johnson, P.S., and Bankey, V., 2009, Geophysical interpretations of the southern Espanola Basin, New Mexico, that contribute to understanding its hydrogeologic framework: U.S. Geological Survey Professional Paper 1761, 88 p.

Green, G.N., and Jones, G.E., 1997, The Digital Geologic Map of New Mexico in ARC/INFO Format: U.S. Geological Survey Open-File Report 97-0052, 9 p.

Heywood, C.E., 1992, Isostatic residual gravity anomalies of New Mexico, U.S. Geological Survey Water-Resources Investigations Report 91-4065, 27 p.

Hinze, W.J., 2003, Bouguer reduction density: why 2.67?: Geophysics, v. 68, p. 1559-1560.

Ingersoll, R.V., Cavazza, W., Baldridge, W.S., and Shafiqullah, M., 1990, Cenozoic sedimentation and paleotectonics of north-central New Mexico: implications for initiation and evolution of the Rio Grande rift: Geological Society of America Bulletin, v. 102, p. 1280-1296.

Ingersoll, R.V., and Cavazza, W., 1991, Reconstruction of Oligo-Miocene volcaniclastic dispersal patterns in north-central New Mexico using sandstone petrofacies: SEPM (Society of for Sedimentary Geology) Special Publication 45, p. 227-236.

Ingersoll, R.V., 2001, Structural and stratigraphic evolution of the Rio Grande rift, northern New Mexico and southern Colorado: International Geology Review, v. 43, p. 867-891.

Jachens, R.W., and Moring, B.C., 1990, Maps of the thickness of Cenozoic deposits and the isostatic residual gravity over basement for Nevada, U.S. Geological Survey Open-File Report 90-404, 15 p.

Jacoby, W., and Smilde, P.L., 2009, Gravity Interpretation: Fundamentals and Application of Gravity Inversion and Geological Interpretation, Springer, 395 p.

Karlstrom, K.E., Amato, J.M., Williams, M.L., Heizler, M., Shaw, C.A., Read, A.S., and Bauer, P.W., 2004, Proterozoic tectonic evolution of the New Mexico region: a synthesis, *in* Mack, G.H., and Giles, K.A., eds., The Geology of New Mexico, New Mexico Geological Society, p. 1-34.

Keller, G.R., Cordell, L., Davis, G.H., Peeples, W.J., and White, G., 1984, A geophysical study of the San Luis basin, *in* Baldridge, W.S., Dickerson, P.W., Riecker, R.E., and Zidek, J., eds., New Mexico Geological Society Guidebook, 35th Field Conference, Rio Grande Rift: Northern New Mexico, p. 51-57.

Keller, G.R., Hildenbrand, T.G., Hinze, W.J., and Li, X., 2006, The quest for the perfect gravity anomaly: Part 2 — Mass effects and anomaly inversion: Society of Exploration Geophysicists Technical Program Expanded Abstracts, v. 25, p. 864.

Kluth, C.F., and Schaftenaar, C.H., 1994, Depth and geometry of the northern Rio Grande rift in the San Luis basin, south-central Colorado, *in* Keller, G.R., and Cather, S.M., eds., Basins of the Rio Grande Rift: Structure, Stratigraphy, and Tectonic Setting: Boulder, Geological Society of America Special Paper 291, p. 27-37.

Large, E., and Ingersoll, R.V., 1997, Miocene and Pliocene petrofacies of the northern Albuquerque basin, New Mexico, and implications for evolution of the Rio Grande rift: Journal of Sedimentary Research, v. 67, p. 462-468.

Lipman, P.W., 1975a, Evolution of the Platoro caldera complex and related volcanic rocks, southeastern San Juan Mountains, Colorado, U.S. Geological Survey Professional Paper 852, p. 128.

—, 1975b, Geologic map of the lower Conejos River canyon area, southeastern San Juan Mountains, Colorado, U.S. Geological Survey Miscellaneous Investigations Map I-901, scale 1:48,000.

Lipman, P.W., and Mehnert, H.H., 1975, Late Cenozoic basaltic volcanism and development of the Rio Grande depression in the southern Rocky Mountains, *in* Curtis, B.F., ed., Cenozoic History of the Southern Rocky Mountains: Geological Society of America Memoir 144, p. 119-154.

—, 1979, The Taos Plateau volcanic field, northern Rio Grande rift, New Mexico, *in* Riecker, R.E., ed., Rio Grande Rift: Tectonics and Magmatism: Washington, D.C., American Geophysical Union, p. 289-311.

Lipman, P.W., 1981, Volcano-tectonic setting of Tertiary ore deposits, southern Rocky Mountains, *in* Dickinson, W.R., and Payne, W.D., eds., Relation of tectonics to ore deposits in the southern Cordillera: Arizona Geological Society Digest, v. 14, p. 199-213.

—, 1983, The Miocene Questa caldera, northern New Mexico: relation to batholith emplacement and associated molybdenum mineralization: The Genesis of Rocky Mountain Ore Deposits: Changes with time and tectonics: Proceedings of the Denver Region Exploration Geologists Society Symposium, p. 133-149.

Lipman, P.W., Mehnert, H.H., and Naeser, C.W., 1986, Evolution of the Latir volcanic field, northern New Mexico, and its relation to the Rio Grande rift, as indicated by potassium-argon and fission track dating: Journal of Geophysical Research, v. 91, p. 6329-6345.

Lipman, P.W., Dungan, M.A., Brown, L.L., and Deino, A., 1996, Recurrent eruption and subsidence at the Platoro caldera complex, southeastern San Juan volcanic field, Colorado: new tales from old tuffs: Geological Society of America Bulletin, v. 108, p. 1039-1055.

Lipman, P.W., 2007, Incremental assembly and prolonged consolidation of Cordilleran magma chambers: evidence from the Southern Rocky mountain volcanic field: Geosphere, v. 3, p. 42-70.
Logsdon, M.J., 1981, A preliminary basin analysis of the El Rito Formation (Eocene), north-central New Mexico: Geological Society of America Bulletin, v. 92, p. 968-975.
Maldonado, F., 2008, Geologic map of the Abiquiu quadrangle, Rio Arriba County, New Mexico: U.S. Geological Survey Scientific Investigations Map 2998, 1:24,000 scale map.
Maldonado, F., and Kelley, S.A., 2009, Revisions to the stratigrpahic nomenclature of the Abiquiu Formation, Abiquiu and contiguous areas, north-central New Mexico: New Mexico Geology, v. 31, p. 3-8.
Manley, K., 1981, Redefinition and description of the Los Pinos Formation of north-central New Mexico: Geological Society of America Bulletin, v. 92, p. 984-989.
—, 1982a, Geologic map of the Bighorn Peak quadrangle, Rio Arriba County, New Mexico and Conejos County, Colorado: U.S. Geological Survey Miscellaneous Field Studies Map MF-1451, 1:24,000 scale map.
—, 1982b, Geologic map of the Broke Off Mountain quadrangle, Rio Arriba County, New Mexico: U.S. Geological Survey Miscellaneous Field Studies Map MF-1450, 1:24,000 scale map.
Manley, K., and Wobus, R.A., 1982, Reconnaissance geologic map of the Mule Canyon quadrangle, Rio Arriba County, New Mexico: U.S. Geological Survey Miscellaneous Field Studies Map MF-1407, 1:24,000 scale map.
—, 1985, Reconnaissance geologic map of the Toltec Mesa quadrangle, Rio Arriba County, New Mexico: U.S. Geological Survey Miscellaneous Field Studies Map MF-1624, 1:24,000 scale map.
Manley, K., Scott, G.R., and Wobus, R.A., 1987, Geologic map of the Aztec 1 degree by 2 degree quadrangle, northwestern New Mexico and southern Colorado: U.S. Geological Survey Miscellaneous Investigations Series Map I-1730, 1:250,000 scale map.
Morgan, P., Seager, W.R., and Golombek, M.P., 1986, Cenozoic thermal, mechanical, and tectonic evolution of the Rio Grande rift: Journal of Geophysical Research, v. 91, p. 6263-6276.
Muehlberger, W.R., 1968, Geology of Brazos Peak Quadrangle, New Mexico: New Mexico Bureau of Mines and Mineral Resources Geologic Map 22.
Ruleman, C., Shroba, R., and Thompson, R.A., 2007, Chapter C - Field Trip Day 3: Quaternary geology of Sunshine Valley and associated neotectonics along the Latir Peaks section of the southern Sangre de Cristo Fault Zone, *in* Machette, M.N., Coates, M.M., and Johnson, M.L., eds., 2007 Rocky Mountain Section Friends of the Pleistocene Field Trip- Quaternary Geology of the San Luis Basin of Colorado and New Mexico, September 7-9, 2007: U.S. Geological Survey Open-File Report 2007-1193, p. 111-133.
Simpson, R.W., Jachens, R.W., Blakely, R.J., and Saltus, R.W., 1986, A new isostatic residual gravity map of the conterminous United States with a discussion on the significance of isostatic residual anomalies: Journal of Geophysical Research, v. 91, p. 8348-8372.
Smith, G.A., Moore, J.D., and McIntosh, W.C., 2002, Assessing roles of volcanism and basin subsidence in causing Oligocene-lower Miocene sedimentation in the northern Rio Grande rift, New Mexico, USA: Journal of Sedimentary Research, v. 72, p. 836-848.
Smith, G.A., 2004, Middle to late Cenozoic development of the Rio Grande rift and adjacent regions in northern New Mexico, *in* Mack, G.H., and Giles, K.A., eds., The Geology of New Mexico, New Mexico Geological Society, p. 331-358.
Spiegel, Z., and Baldwin, B., 1963, Geology and Water Resources of the Santa Fe Area, New Mexico: U.S. Geological Survey Water-Supply Paper 1525, 258 p.
Telford, W.M., Geldart, L.P., and Sheriff, R.E., 1990, Applied Geophysics, 2nd Ed., Cambridge University Press, 770 p.
Thompson, R.A., and Dungan, M.A., 1985, The petrology and geochemistry of the Handkerchief Mesa mixed magma complex, San Juan Mountains, Colorado: Journal of Volcanology and Geothermal Research, v. 26, p. 251-274.
Thompson, R.A., and Machette, M.N., 1989, Geologic map of the San Luis Hills area, Conejos and Costilla Counties, Colorado, U.S. Geological Survey Miscellaneous Investigations Map I-1906, scale 1:50,000.
Thompson, R.A., Johnson, C.M., and Mehnert, H.H., 1991, Oligocene basaltic volcanism of the northern Rio Grande rift: San Luis Hills, Colorado: Journal of Geophysical Research, v. 96, p. 13577-13592.
Thompson, R.A., and Lipman, P.W., 1994a, Geologic map of the Los Pinos quadrangle, Rio Arriba and Taos Counties, New Mexico, and Conejos County, Colorado, U.S. Geological Survey Map GQ-1749, scale 1:24,000.
—, 1994b, Geologic map of the San Antonio Mountain quadrangle, Rio Arriba County, New Mexico, U.S. Geological Survey Map GQ-1750, scale 1:24,000.
Tweto, O., 1979, The Rio Grande rift system in Colorado, *in* Riecker, R.E., ed., Rio Grande Rift: Tectonics and Magmatism: Washington, D.C., American Geophysical Union, p. 33-56.
Williams, M.L., 1991, Heterogeneous deformation in a ductile fold-thrust belt: the Proterozoic structural history of the Tusas Mountains, New Mexico: Geological Society of America Bulletin, v. 103, p. 171-188.
Wobus, R.A., and Manley, K., 1982, Reconnaissance geologic map of the Burned Mountain quadrangle, Rio Arriba County, New Mexico: U.S. Geological Survey Miscellaneous Field Studies Map MF-1409, 1:24,000 scale map.